INTERNATIONAL JOURNAL OF
COASTAL & OFFSHORE ENGINEERING
IJCOE Vol.5/No. 3/Fall 2020 (49-56)

Available online at: www. Ijcoe.org

A Parametric Study of Critical Buckling Force in Snaked Lay Pipelines under HP/HT Condition

Yasaman Rezaie[1], Seyed Mohammad Hossein Sharifi[2*], Gholam Reza Rashed[3], Farzad Numani[4]

[1] Master Student of Mechanical Engineering, Petroleum University of Technology; yasaman.rezaie@afp.put.ac.ir
[2]Assistant Professor of Mechanical Engineering Department, Petroleum University of Technology; sharifi@put.ac.ir*
[3]Asociated Professor of Mechanical Engineering Department, Petroleum University of Technology; g.rashed@put.ac.ir
[4]Head of Plant Inspection, Iranian Offshore Oil Company; Fnumani@iooc.co.ir

ARTICLE INFO

Article History:
Received: 16 Mar. 2020
Accepted: 20 Feb. 2021

Keywords:
Offshore Pipeline
Snake Lay Configuration
Lateral Buckling
Critical Buckling Force
High Pressure/ High Temperature

ABSTRACT

Pipelines are an economical way for offshore oil and gas transportation. In operation conditions, flowing high pressure/high temperature (HP/HT) fluids may induce axial expansion. If this expansion is constrained, axial stresses will be created and they may cause pipeline buckling. In order to reduce damages and avoid buckling in unpredictable places, the controlled buckling concept is introduced. To use this concept in the present study, buckling is triggered at some predetermined locations by using the snaked laying method. This paper analyzes the global buckling process of a pipeline by using numerical simulation methods and the effects of loading (internal pressure and temperature) and section properties (diameter and thickness) are investigated on the critical buckling force of snaked lay pipelines under HP/HT conditions. Then, the analysis results of the finite element method (FEM) are compared with analytical solutions and previous simulation methods. This work includes performing nonlinear finite element analysis and modeling pipe-soil interaction of as-laid pipelines by the use of spring elements. The results show that the use of equivalent temperature instead of pressure difference, as already applied in previous studies, is not an authentic method and cannot introduce an accurate outcome. The analysis shows that by increasing pressure and decreasing temperature, the critical buckling force is decreased and the pipeline buckling occurs sooner. The investigation of section properties indicates that the most effective parameter is thickness. It is remarkable to know that at low values of thickness, the effect of diameter is negligible and by increasing thickness, the influence of diameter is increased. Comparing the analytical and numerical results reveals that at low values of circumferential stiffness (ratio of diameter to thickness), there are minor differences between numerical and analytical results.

1. Introduction

Submarine pipelines are one of the most efficient devices for oil and gas transportation. In operational conditions, the pipelines are subjected to high pressure/ high temperature (HP/HT) fluids to ensure the smooth flowing of oil [1]. The HP/HT conditions of hydrocarbon contents in pipelines establish longitudinal expansions. This expansion is limited by the pipe-soil interaction and end connections of the pipeline, resulting in compression forces [2]. Buckling occurs when the effective axial compressive force is increased to a critical load beyond which the pipeline becomes unstable and deforms to reduce compressive load and take a lower energy state. The buckling activation can damage the pipeline integrity and have unfavorable results [3].

There are two different methods to prevent inappropriate effects of lateral buckling: (a) totally constrained method, and (b) controlled lateral buckling concept. In the former method, the pipeline configuration is restricted and the pipeline movements are stopped in any direction, which is possible by trenching, burying and rock dumping, but these solutions are not economical. In contrast, the latter method, which is suggested to work with pipeline rather than operating against it, is much more cost-

effective. To be more specific, lateral buckling is triggered at a number of controlled buckle locations to prevent severe buckles occurring at a few random sites [4]. Some of the methods used in practice to control the number of buckles are terrain irregularities, vertical triggers, and snake lay which are described in more detail in [4]. The snake laying method is the most economical compared to the other suggested means. The main difference between this method and the vertical trigger is that there are no resulting spans and consequently no vortex-induced vibrations (VIV) or trawl hooking loads [2]. To understand the benefits of the snake laying method, Li et al. [5], Liu et al. [6], and Jiang Gung et al. [7] have compared various studies to reveal the advantages of this technique.

There are some successful projects, e.g. the Penguins project [8] and the Echo Yodel project [9], in which the snaked laying method has been used in practice. Preston et al. [10] presented a summary of accepted methodology and performed some analyses to specify an acceptable as-laid pipeline geometry. Rundsag et al. [4] and Rathbone et al. [11] implemented a parametric study to investigate the effect of snake lay geometry on the buckle initiation force, resulting bending moment, and strain by the finite element (FE) software ABAQUS. The investigated parameters included lay radius, arc length, and offset angle. Cumming and Rathbone [12] studied the relationship between the minimum buckle initiation force and the horizontal offset angle of a pipeline, considering an Euler buckling approach. In the end, a relationship is proposed that estimates the buckle initiation force based on pipeline stiffness and weight, offset angle, and friction factor which is then compared against idealized finite element models. Obele Ifena [13] studied the influence of pipe-soil interaction on the design of surface laid subsea pipelines susceptible to lateral buckling. Liu et al. [14] suggested a new configuration for curved section of snaked laying method. It is recommended to use a sinusoidal configuration instead of circular sections which can reduce the buckle initiation force. Wang et al. [2] proposed a new shape of snaked laying curve based on a combination of genetic algorithm (GA) and finite element analysis.

There are some basic analytical methods introduced many years ago. In 1984, Hobbs [15] suggested four models for lateral global buckling and obtained an analytical solution for buckling force, buckling length, and buckling deformation amplitude. In another study, Taylor and Gan [16] researched pipelines with imperfections and obtained analytical solutions which include the first and second order for a buckling model. All the studies mentioned above have addressed pipelines that experienced high temperatures, but they have overlooked the effect of external and internal pressures. More specifically, the effect of the pressure difference has been converted into an equivalent temperature difference, as explained in more detail in [17] and [18]. Besides, most parametric studies have focused on the snake laying geometry and the effect of the pipeline section has not been investigated.

The present study focuses on the assessment of critical buckling force F_{cr} (or the buckle initiator force) by considering the effects of the hydrostatic pressure and internal pressure of fluid contents. In the next step, the effects of external diameter and thickness are analyzed to establish how variations in pipeline section properties will influence the buckle initiation force.

2. Finite Element Modeling

The finite element method presents an appropriate way to assess the lateral buckling of pipelines. The finite element model of a subsea pipeline is described in detail on the basis of four aspects.

2.1. Configuration of Snaked Lay Pipelines

A typical configuration of snaked-lay pipelines composed of a straight section and a curved section is shown in Figure 1. The straight section is usually longer than the curve one and it can be described by L, V and β called laying wavelength, amplitude curvature, and laying chord length, respectively. In this figure, “ab”, “de”, “ef”, and “hi” are examples of the straight section. The configuration of a typical arc curve section is described in more detail in which the lay radius R and the offset angle θ control the shape of the curve section. Examples of the curved section include “bcd” and “fgh”. It is significant to know that the relationship between the lay radius, offset angle, and laying chord length can be expressed by Eq. (1):

$$\beta = R \times \theta \tag{1}$$

In this study, just three parameters, i.e. V, R, and θ, are used for simulation and these are equal to 26.25 m, 287.5 m, and 5.38. The purpose of choosing these values is to be ensuring that the third mode of buckling will happen. More detail about this mode are provided in the next sections. Because of symmetric loading and geometry, just a quarter of pipeline length is simulated in Figure 1, i.e. “cde”.

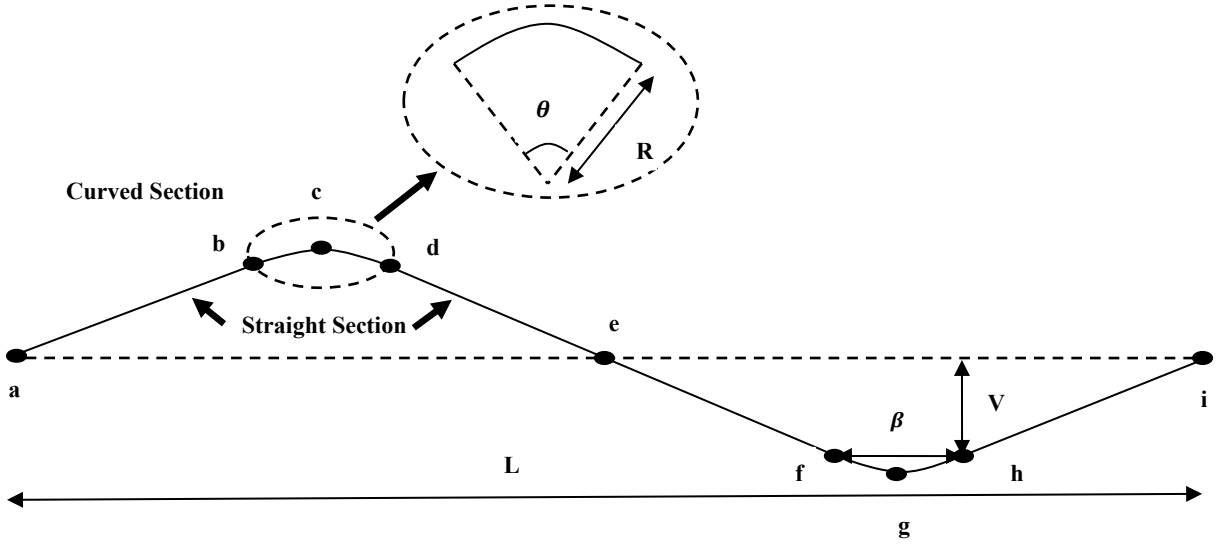

Figure 1. The snake lay configuration

2.2. Pipeline Properties

The inputs for material properties include basic data such as Young's modulus, Poisson's ratio, thermal expansion coefficient, and yield strength, which are listed in Table 1. The carbon steel material used for the pipe is API 5L grade X65.

Table 1. The material properties of pipeline [19]

Characteristic	Value
Elasticity modulus (E_{steel})	2.07×10^{11} $[N\ m^{-2}]$
Poisson's ratio (ν)	0.3 [-]
Thermal expansion coefficient (α)	1.1×10^{-5} $[℃^{-1}]$
Yield stress	545 $[MPa]$
Density (ρ)	**7850** $[\frac{Kg}{m^3}]$

The isotropic power law is adopted to describe the pipeline material behavior as expressed in more detail by Eq. (2):

$$\sigma = \begin{cases} E\varepsilon & \varepsilon \le \varepsilon_y \\ \sigma_0 (\frac{\varepsilon}{\varepsilon_y})^n & \varepsilon > \varepsilon_y \end{cases} \quad (2)$$

where σ_0 is the yield stress, n is the strain hardening assumed to be 0.05, and ε_y is the yield strain, which is equal to 0.00263. 3D-finite element simulations were performed using the ABAQUS standard code [20]. The pipe was modeled using eight-node 3D elements (C3D8R).

2.3. Pipe-Soil Interaction

In this research, submerged weight is considered. The presence of this loading introduces self-weight on each element of the pipeline and consequently creates an interaction between pipeline and soil. The simulation of this contact can be performed by using SPRING1 elements in order to consider axial, lateral and normal interactions as shown in Figure 2.

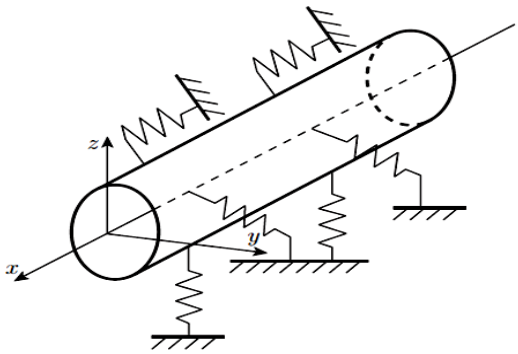

Figure 2. The pipe-soil interaction model by using SPRING elements [14]

SPRING1 is placed between the seabed and outer pipe nodes and acts in a fixed determined direction. Bi-linear and tri-linear resistance models are selected for axial and lateral pipe-soil interactions, respectively. For normal interaction, it is assumed that the spring has high values of stiffness in order to prevent the motion of the pipeline in this direction. The basic parameters for the description of resistance models are listed in Table 2.

Table 2. The basic parameters for the pipe-soil interaction [11]

Characteristic	Value
Axial break out displacement	10 $[mm]$
Axial friction coefficient	0.6 [-]
Lateral break out displacement	140 $[mm]$
Peak lateral friction coefficient	1.1 [-]
Residual lateral displacement	990 $[\boldsymbol{mm}]$
Residual lateral friction coefficient	0.6 [-]

2.4. Pipeline Loading

A 3D model is used to simulate the pipeline global buckling behavior. Disregarding the wave-current load and residual lay tension associated with the installation, five main forces act on a pipeline including hydrostatic pressure, the submerged weight of the pipeline, internal pressure, soil resistance, and temperature load [1]. The loading and boundary conditions of a part of the pipeline are shown in Figure 3.

3. Analytical Solution for Snake Laid Pipelines

Rathbone et al. [11] proposed a formula for calculating the critical buckling force, F_{cr}, of a curved pipeline with lay radius, R. To derive this equation, it is assumed that the pipeline deflection happens when the axial compression force exceeds the lateral soil resistance.
The relationship between critical buckling force, lateral resistance, and lay radius can be expressed as:

$$F_{cr} = \mu . W_{sub} . R \qquad (3)$$

where W_{sub} and μ are the submerged weight and lateral friction factor, respectively.

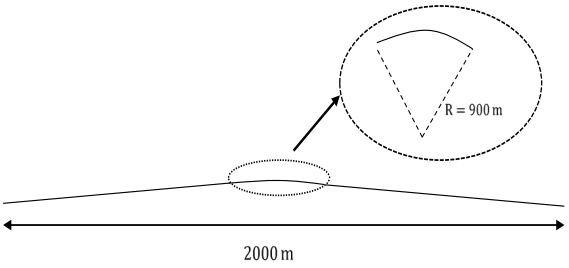

Figure 4. The geometric shape of pipeline

The axial compressive force of the pipelines with $\theta = 4°$ and $\theta = 2°$ are calculated in this section. It is important to know that the main difference between the present study and Rathbone et al. [11] is that the work introduced here is done in a 3D environment whereas Rathbone et al.'s study in a 2D environment.
Figure 5 shows the relationship between the axial compressive force and the value of displacement in the midpoint of the pipeline. The peak point of the curve shows the value of the buckle initiation force. Before this point, the pre-buckling stage happens and it can be seen that the axial compressive force increases with small variations in displacement. After the compressive force touches the peak point, the post

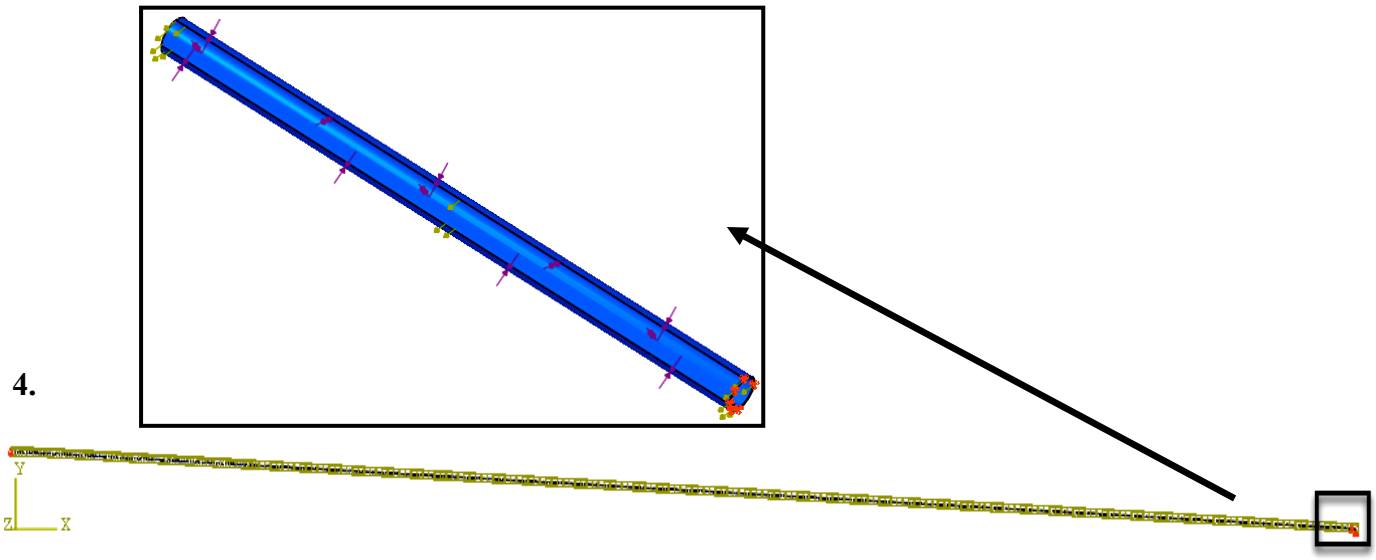

Figure 3. Close up view of loading and boundary condition of part of pipeline length

4. Verification

The same pipeline in Rathbone et al. [11] is selected to verify the proposed finite element model. The pipeline section properties, i.e. outside diameter and thickness, are equal to 508 mm and 23.1 mm, respectively. The geometric shape of the pipeline is shown in Figure 4.

buckling stage happens and it decreases quickly. As shown in Figure 5, the buckle initiation forces with $\theta = 4°$ and $\theta = 2°$ are 1.71 MN and 1.91 MN, respectively. The critical buckling forces in Rathbone et al. [11] are 1.738 MN and 1.966 MN and the relative error are 2.8% and 5.6%, respectively. Therefore, the proposed finite element model in this research can reach the true critical buckling force of snaked-lay pipelines.

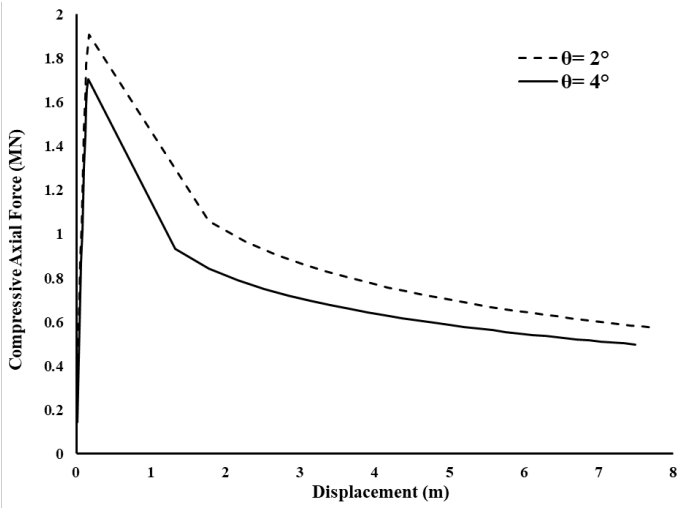

Figure 5. The axial compressive force versus the midpoint pipeline buckling amplitude

5. Factors Influencing the Initiation Force

In pipeline lateral global buckling analysis, there are several effective parameters investigated in this paper: thickness t, diameter D, internal pressure P, and temperature difference T. Obviously, these factors will affect the initiation force. The impact of these factors is revealed in the following analyses.

5.1. Internal Pressure and Temperature of Pipeline Content

Different combinations of pressures and temperatures are compared here. It is important to note that the value of hydrostatic pressure is fixed and it is equal to $1\ MPa$ to simulate the depth of $100\ m$. Figure 6 illustrates the resulting buckle shape from a full non-linear FE analysis that has been plotted for various temperature steps.

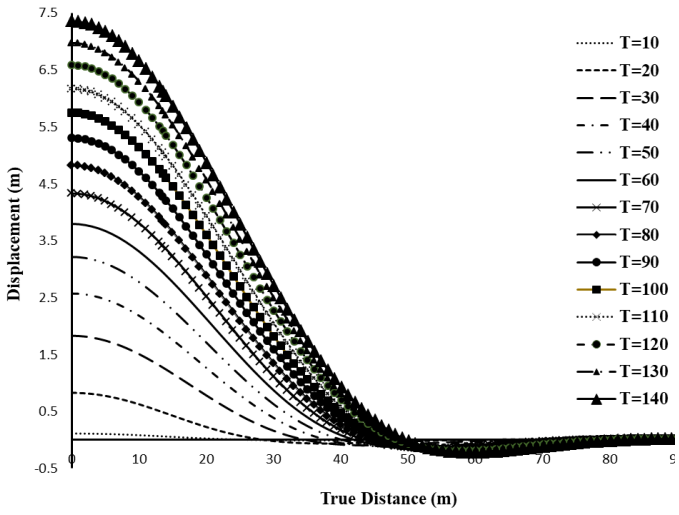

Figure 6. The buckle shape

It can be seen that about $90\ m$ of the investigated pipeline experienced buckling and the value of displacement grew with the increase in temperature. According to the lateral buckling mode shapes proposed by Hobbs [15], it is obvious that this pipeline is in mode 3. It should be noted that this figure displays the lateral displacement of a quarter of the pipeline starting from point zero on the horizontal axis.

In this study, three different temperatures are considered, i.e. 70℃, 120℃ and 170 ℃. The combination of each temperature with three different pressures, including $10\ MPa$, $20 MPa$ and $30\ MPa$, are investigated. It is significant to know that the values indicated for pressures are the difference between internal and external pressure. In this analysis, it is assumed that the section properties are fixed and the values of diameter and thickness are equal to $345\ mm$ and $16.195\ mm$, respectively. The results of this investigation are shown in Figures 7-9.

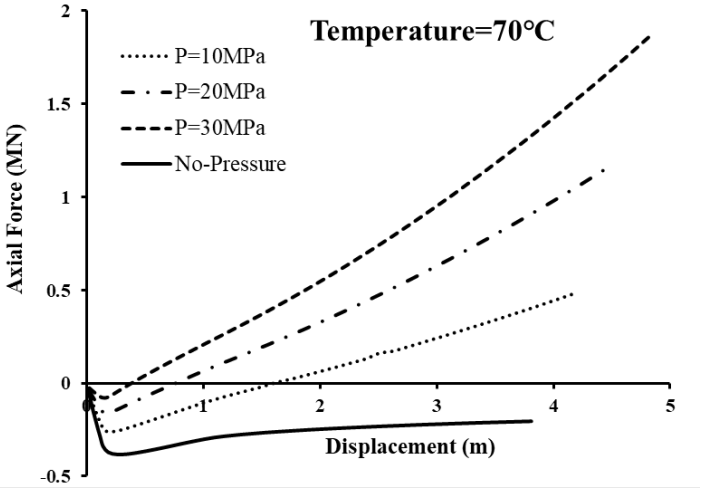

Figure 7. The change curve of buckling force for $T = 70$℃

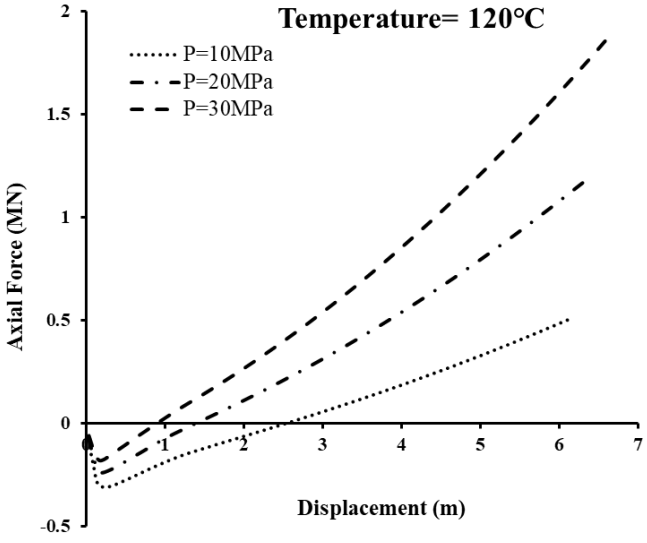

Figure 8. The change curve of buckling force for $T = 120$℃

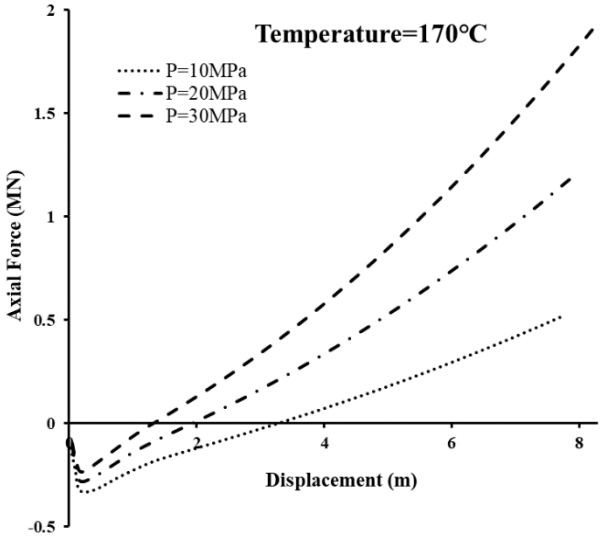

Figure 9. The change curve of buckling force for $T = 170$℃

In Figure 7, there are four curves, one of which is plotted for a condition in that external and internal pressures are not simulated. In order to have more accurate comparisons between the presented results, the initiation force of each curve is reported in Table 3.

Table 3. The comparison of the initiation force

Temperature difference (ΔT) [℃]	Pressure difference (ΔP) [MPa]	Compressive axial force [MN]
70	10	0.2585
	20	0.1581
	30	0.0776
120	10	0.3113
	20	0.2402
	30	0.1817
170	10	0.3241
	20	0.2799
	30	0.2349

The analysis of the results shows that:

a) By considering a fixed pressure difference, the compressive axial force is increased with the increase in temperature. In other words, at high temperatures, buckling occurs later. For example, if the pressure difference is assumed to be 30 MPa, the value of the critical axial force is increased by about 15% when the temperature varies from 70℃ to 170℃.

b) By assuming a fixed temperature difference, the buckling initiation force is decreased with the increase in pressure. To be more specific, buckling occurs sooner at high values of pressure. For example, if the temperature of the contents is considered 70℃, it can be seen that the value of the compressive axial force is decreased by about 18%, while the pressure varies from 10 MPa to 30 MPa.

In order to explain the two cases observed above in more detail, it is necessary to analyze pipeline forces more accurately, so the effect of pressure and temperature are described separately. When the pipeline is exposed to internal pressure, tensile stress develops in a hoop direction. Due to Poisson's effect, this hoop stress will tend to shorten the pipeline. Since this shortening is prevented by end constraints, the tensile stresses are increased. But, the effect of temperature is different, and the axial force gets into compression due to the thermal expansion when the pipeline is not allowed to move axially [21]. Since the final compressive axial force is a combination of temperature and pressure effects, an increase in the pressure will increase the tension stresses and consequently, it will decrease the compressive axial force, which is in agreement with obtained results but the temperature will build up the compressive axial force as supported by this study.

As shown in Figure 7, when the pressure difference is not simulated, buckling occurs at $0.3826\ MN$. By comparing this value with the initiation forces of Table 3, it is concluded that neglecting the effects of external and internal pressure is not a reasonable assumption and introduces imprecise results that are not useful in practical conditions.

For the pipeline analyzed in this section, the compressive axial force is calculated by Eq. (3) and the obtained value is compared with the FE results. Since the only effective parameters in the suggested equation are lateral friction factor, submerged weight, and lay radius and they are not influenced by pressure and temperature differences, the compressive axial force is fixed and it is equal to $0.349 MPa$. The maximum difference between analytical and numerical results is occurred in (70℃ , 30 MPa) which is about 27% and the minimum is occurred in (170℃ , 10 MPa) and it is equal to 2.5%. It is necessary to remind that in this study, friction factor is considered in lateral, axial and normal directions while lateral friction factor is the only effective parameter in Eq.(3) and other directions are ignored.

5.2. Effect of Pipeline Section Dimension

The pipeline section characteristics specify the flexural rigidity and influence stress and deformation [1]. Figures 10 and 11 illustrate the critical buckling force of the pipelines with different section dimensions by considering the temperature of 100 ℃ and pressure of 20 MPa.

In Figure 10, the effect of thickness is investigated and the buckling force curve is plotted by considering three different values of diameter. The results of FE simulations are compared with Eq. (3). In this section, the buckling force of Eq. (3) is not constant because the variation in thickness and diameter will influence the submerged weight.

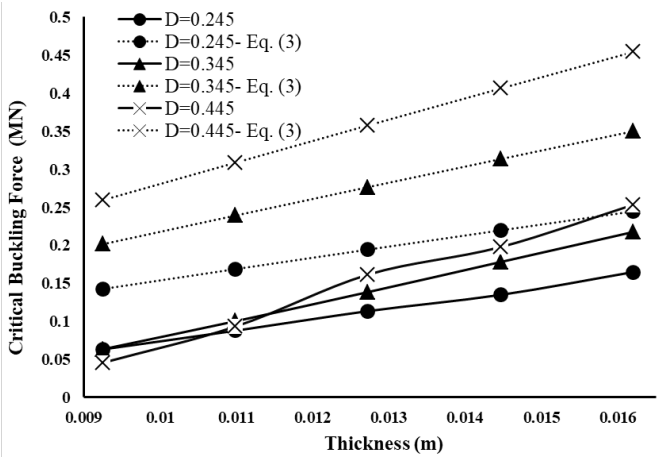

Figure 10. The critical buckling force of the pipelines for different thicknesses

It can be seen in Figure 10 that changes in t have a considerable effect on the critical buckling force so that with the increase in thickness, the critical buckling force is increased. Comparing the results of FE simulations with Eq. (3) illustrates that by increasing thickness, the differences between numerical and analytical results are approximately fixed and by growing diameter, it is increased. To be more specific, at low and high values of circumferential stiffness (ratio of diameter to thickness), differences are about 7% and 21%, respectively which minimum difference is occurred in diameter of 0.245 m and thickness of 0.00925 and maximum difference is occurred in diameter of 0.445 m and thickness of 0.016195.

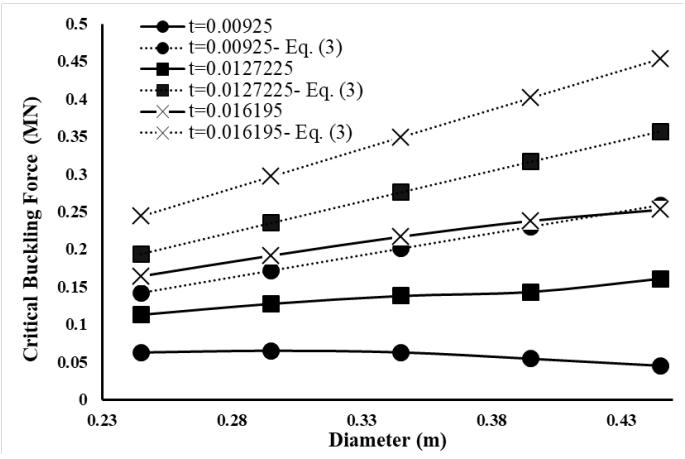

Figure 11. The critical buckling force of the pipelines for different diameters

It can be seen in Figure 11 that at lower thicknesses, changes in D does not have a considerable effect on the critical buckling force, but with the increase in thickness, the effect of diameter is increased and the critical buckling force grows. The differences between the analytical and numerical results increased with the increase in circumferential stiffness.

As a general conclusion, it was observed that by increasing thickness and diameter, the critical buckling force is increased and buckling happens later. This effect can be explained by the buckling behavior of beams and the value of critical buckling force is increased with the increase in the moment of inertia.

It is obvious that the numerical method yielded more conservative results versus the analytical method in both Figure 10 and Figure 11.

6. Conclusions

Deep offshore pipelines undergo lateral global buckling because of the HP/HT condition. The use of controlled lateral buckling methods such as snaked lay configuration triggers buckle at some predetermined locations. The common characteristic for the controlled lateral buckling is to reduce the buckle initiation force at the selected locations because in this condition the probability of buckling at the locations is increased and the rogue random buckles are prevented .

This paper investigated the effects of HP/HT loading and section properties on critical buckling force and compared analytical and numerical results. The main conclusions are as follows:

- The critical buckling force is increased with an increase in temperature and it is decreased with an increase in pressure. So, to increase the probability of buckling, the pipeline should experience higher pressures and lower temperatures.
- In most previous studies, it has been assumed that the effect of pressure difference can be equivalent to the temperature difference and it has the same effect, but this paper shows that there are significant differences between the obtained results, and the maximum value of this difference is reported at about 30.5% which is occurred in temperature and pressure difference of (70 ℃, 30 MPa).
- Critical buckling force is increased with an increase in diameter and thickness although changes in thickness have more considerable effects than the diameter.
- Comparing the results of the analytical and FE method illustrates that the proposed equation cannot calculate the critical buckling force with good accuracy and in most investigations, it experiences considerable differences with numerical results which are reported to be about 27%.

7. Acknowledgment

The authors are grateful for the support of the Iranian Offshore Oil Company (IOOC).

8. References

1- Z. Hong, R. Liu, W. Liu, and S. Yan, (2015), *A lateral global buckling failure envelope for a high temperature and high pressure (HT/HP) submarine pipeline*, Applied Ocean Research, Vol. 51, p. 117-128.

2- Z. Wang, Z. Chen, Y. He, and H. Liu, (2015), *Optimized configuration of snaked-lay subsea pipelines for controlled lateral buckling method*, in The Twenty-fifth International Ocean and Polar Engineering Conference.

3- D. Bruton, M. Carr, M. Crawford, and E. Poiate, (2005), *The safe design of hot on-bottom pipelines with lateral buckling using the design guideline developed by the safebuck joint industry project*, in Proceedings of the Deep Offshore Technology Conference, Vitoria, Espirito Santo, Brazil.

4- J. O. Rundsag, K. Tørnes, G. Cumming, A. D. Rathbone, and C. Roberts, (2008), *Optimised Snaked Lay Geometry*., in Eighteenth International Offshore and Polar Engineering Conference, International Society of Offshore and Polar Engineers.

5- Z.-G. Li, C. Wang, N. He, and D.-Y. Zhao, (2008), *An overview of deepwater pipeline laying technology*, *China Ocean Engineering,* Vol. 22, no. 3,p. 521-532.

6- W. Liu and J. Fu, (2018), *Global Buckling Behavior of Snaked-Laid and Straight Laid Subsea Pipelines*, in the 28th International Ocean and Polar Engineering Conference.

7- J. Guan, P. R. Nystrom, and H. F. Hansen, (2007), *Optimized solutions to control lateral buckling of pipelines with snaked-lay: theoretical and numerical studies*, in ASME 2007 26th International Conference on Offshore Mechanics and Arctic Engineering.

8- I. Matheson, M. Carr, R. Peek, P. Saunders, and N. George, (2008), *Penguins flowline lateral buckle formation analysis and verification*, in ASME 2004 23rd International Conference on Offshore Mechanics and Arctic Engineering.

9- M. Wagstaff, (2003), *Detailed design and operational performance assessment of pipeline buckle initiators to mitigate lateral buckling*, in Proceedings of the Petromin Pipeline Conference, Singapore.

10- R. Preston, F. Drennan, and C. Cameron, (1999), *Controlled lateral buckling of large diameter pipeline by snaked lay*, in The Ninth International Offshore and Polar Engineering Conference.

11- A. Rathbone, K. Tørnes, G. Cumming, C. Roberts, and J. Rundsag, (2008), *Effect of lateral pipelay imperfections on global buckling design*, in The Eighteenth International Offshore and Polar Engineering Conference.

12- G. Cumming and A. Rathbone, (2010), *Euler buckling of idealised horizontal pipeline imperfections*, in ASME 2010 29th International Conference on Ocean, Offshore and Arctic Engineering.

13- I. Obele, (2013), *Lateral buckling and axial walking of surface laid subsea pipeline*, Master's thesis, University of Stavanger, Norway.

14- Y. Liu, X. Li, and J. Zhou, (2013), *Post-buckling studies on snaked-lay pipeline with new shape*, Journal of information & computational science, Vol. 9(12), p. 3315-24.

15- R. E. Hobbs, (1984), *In-service buckling of heated pipelines*, Journal of Transportation Engineering., Vol. 110(2), p.175-89.

16- N. Taylor and A. Gan, (1986), *Refined modelling for the lateral buckling of submarine pipelines*, Journal of Constructional Steel Research, Vol. 6(2), p.143-62.

17- H. Karampour, F. Albermani, and J. Gross, (2013), *On lateral and upheaval buckling of subsea pipelines*, Engineering structures, Vol. 52, p.317-330.

18- Z. Hong, R. Liu, W. Liu, and S. Yan, (2015), *Study on lateral buckling characteristics of a submarine pipeline with a single arch symmetric initial imperfection*, Ocean engineering, Vol. 108, p.21-32.

19- Y. Zhang, D. Yi, Z. Xiao, and Z. Huang, (2015), *Engineering critical assessment for offshore pipelines with 3-D elliptical embedded cracks*, Engineering Failure Analysis, Vol. 51(1), p.37-54.

20- Hibbitt, Karlsson, and Sorensen, (2013), ABAQUS/STANDARD. User's Guide and Theoretical Manual, Version 6.13, 2013.

21- O. Fyrileiv and L. Collberg, (2005), *Influence of pressure in pipeline design: effective axial force*, in ASME 2005 24th International Conference on Offshore Mechanics and Arctic Engineering.